

Neuronal Fragile X Mental Retardation Protein activates glial insulin receptor mediated PDF-Tri  
neuron developmental clearance

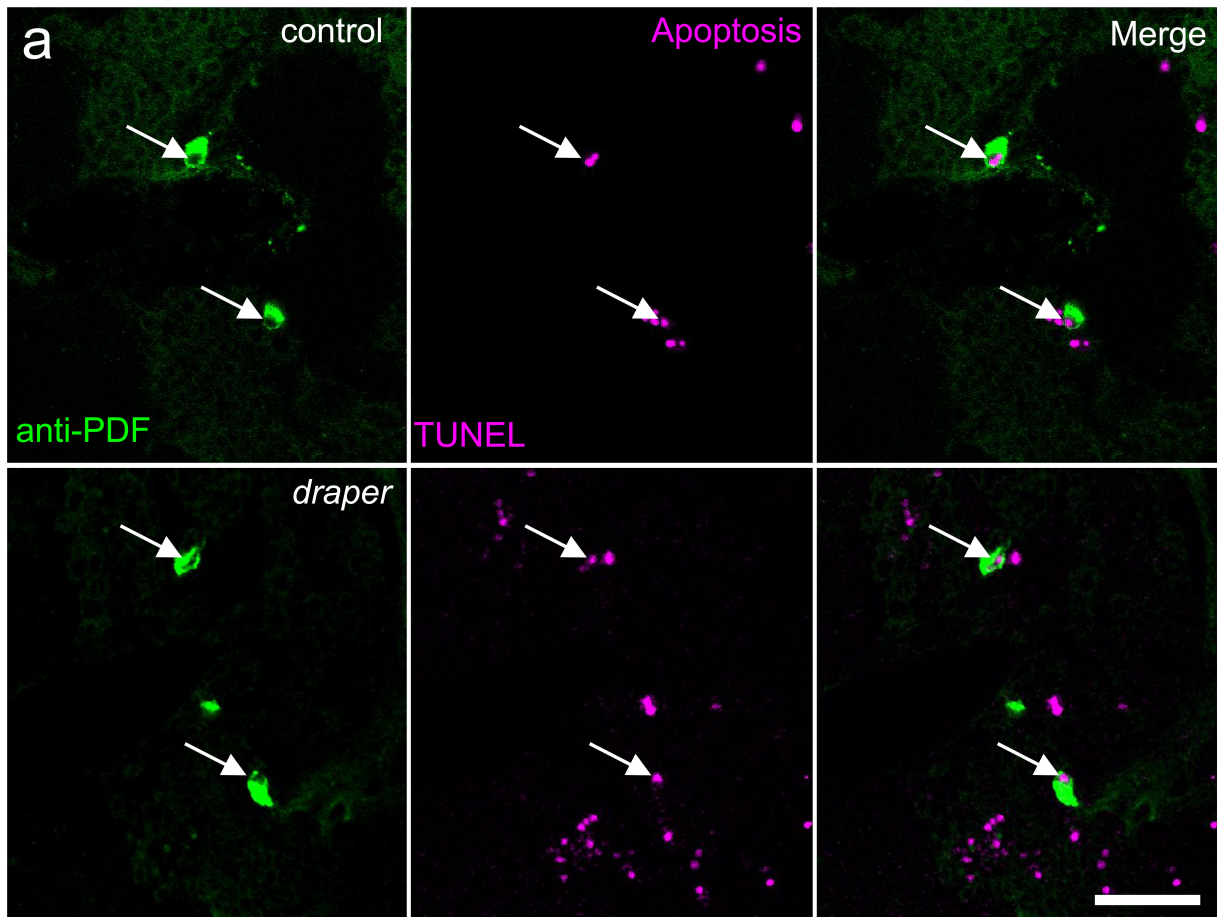
Dominic J. Vita<sup>1</sup>, Cole J. Meier<sup>1</sup> and Kendal Broadie<sup>1,2,3\*</sup>

<sup>1</sup>Department of Biological Sciences, Vanderbilt University, Nashville, Tennessee, 37235, USA

<sup>2</sup>Kennedy Center for Research on Human Development, Nashville, Tennessee 37235, USA

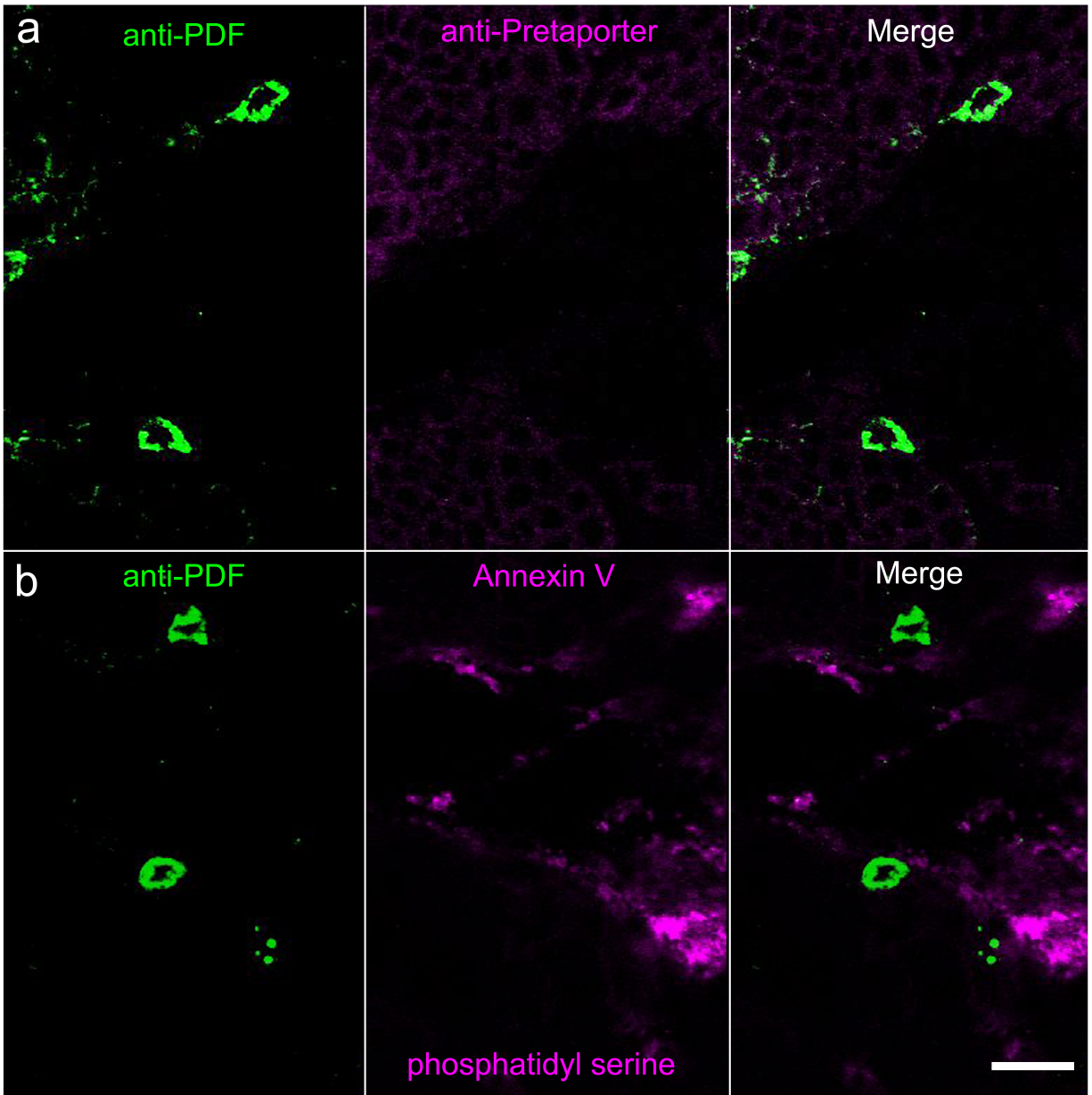
<sup>3</sup>Vanderbilt Brain Institute, Vanderbilt University Medical Center, Nashville, Tennessee, 37235, USA

Supplemental Data



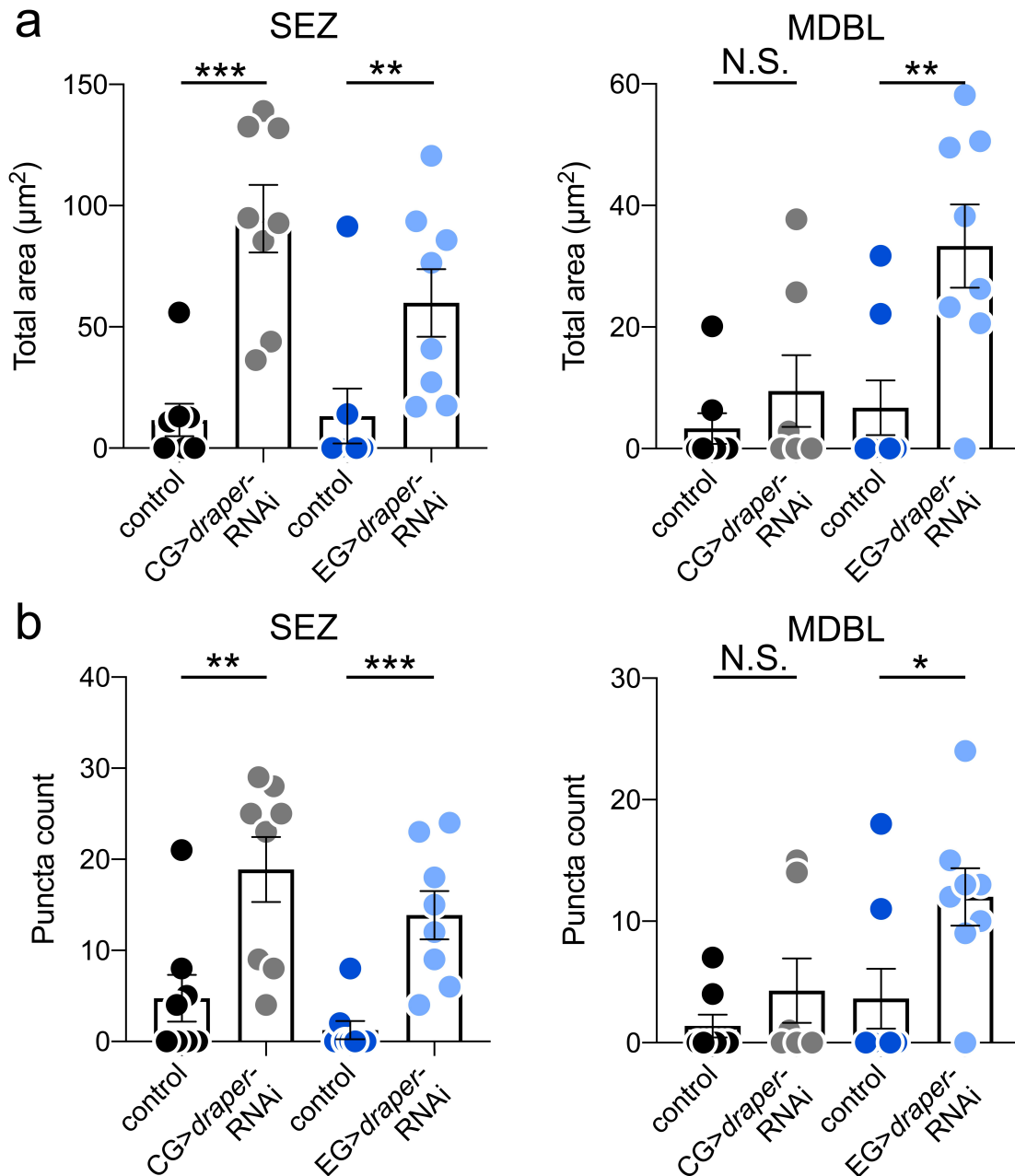
Supplemental Figure 1: *draper* null mutants show TUNEL-positive PDF-Tri neuron apoptosis

a. Representative central brain PDF-Tri region images (0 DPE) labeled with anti-PDF (green, left), TUNEL (magenta, middle) and the merge (right) in control (*w<sup>1118</sup>*, top) and *draper* null mutant (*draper<sup>A5</sup>*, bottom). Arrows indicate TUNEL positive PDF-Tri neuron cell bodies. Scale bar: 25 $\mu$ m. b. Quantification of the total number of PDF-Tri neuron cell bodies (left) and the percentage of TUNEL positive PDF-Tri neurons (right). Box and whisker plots show quartiles with max and min values, with plus sign indicating the mean. Total PDF-Tri neurons: Two-sided Mann-Whitney,  $p=0.763$ ,  $0.878\pm 0.0551$   $n=15$  control,  $0.875\pm 0.0897$   $n=12$  *draper*. TUNEL positive neurons: Two-sided Mann-Whitney,  $p=0.227$ ,  $2.333\pm 0.1260$   $n=15$  control,  $2.000\pm 0.213$   $n=12$  *draper*. Sample size is  $n$ =number of animals. Significance:  $p>0.05$  (not significant, N.S.). Source data for this figure are provided in Source Data file.



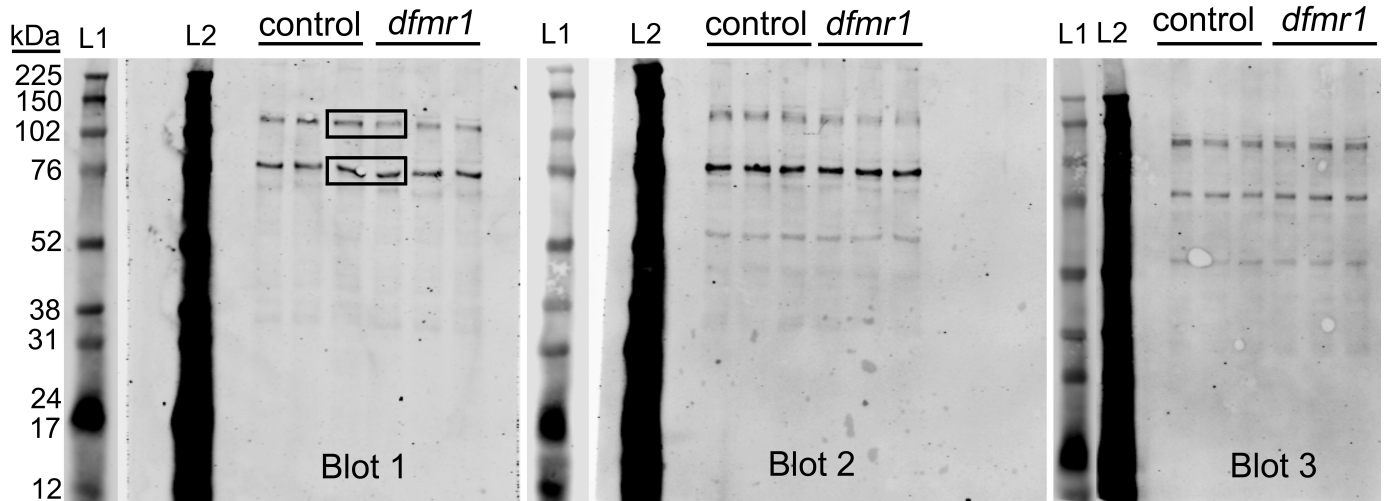
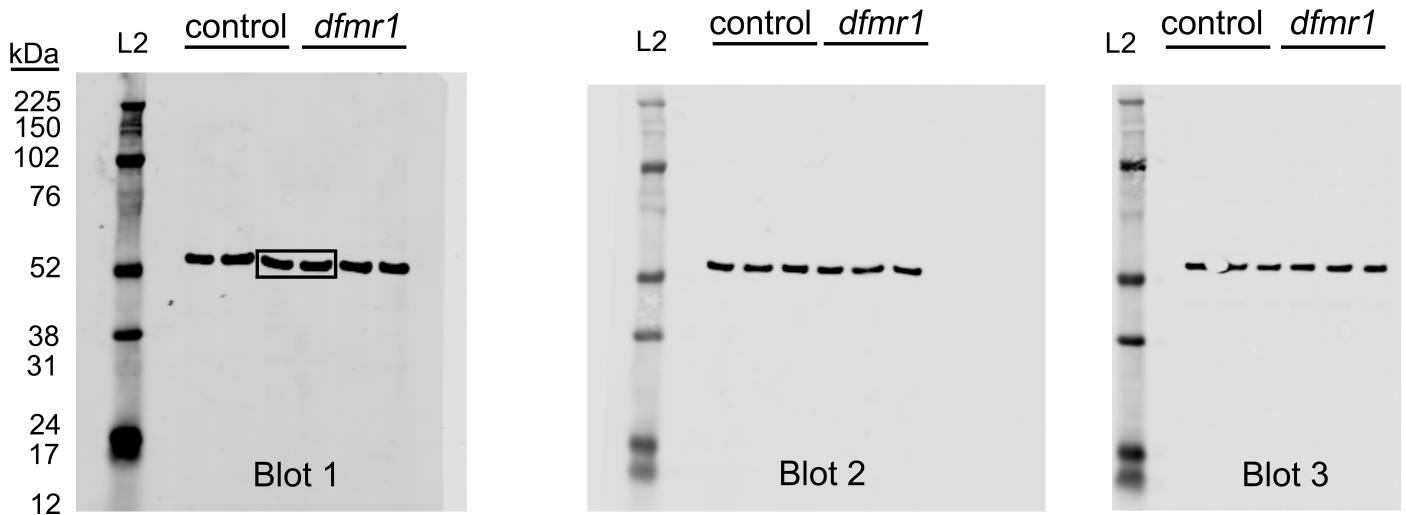
Supplemental Figure 2: PDF-Tri neurons lack candidate cell death/phagocytosis markers

a. Representative central brain PDF-Tri region images (0 DPE) labeled with anti-PDF (green, left), anti-Pretauporter (magenta, middle), and the merge (right). No enrichment is observed in PDF-Tri neurons. b. The same brain regions labeled for anti-PDF (green, left), phosphatidylserine (Annexin V, magenta, middle), and the merge (right). No enrichment is observed within PDF-Tri neurons. Scale bar: 10 $\mu$ m. Images are representative of two independent experiments.



Supplemental Figure 3: Glial class PDF-Tri neuron clearance in spatially restricted domains

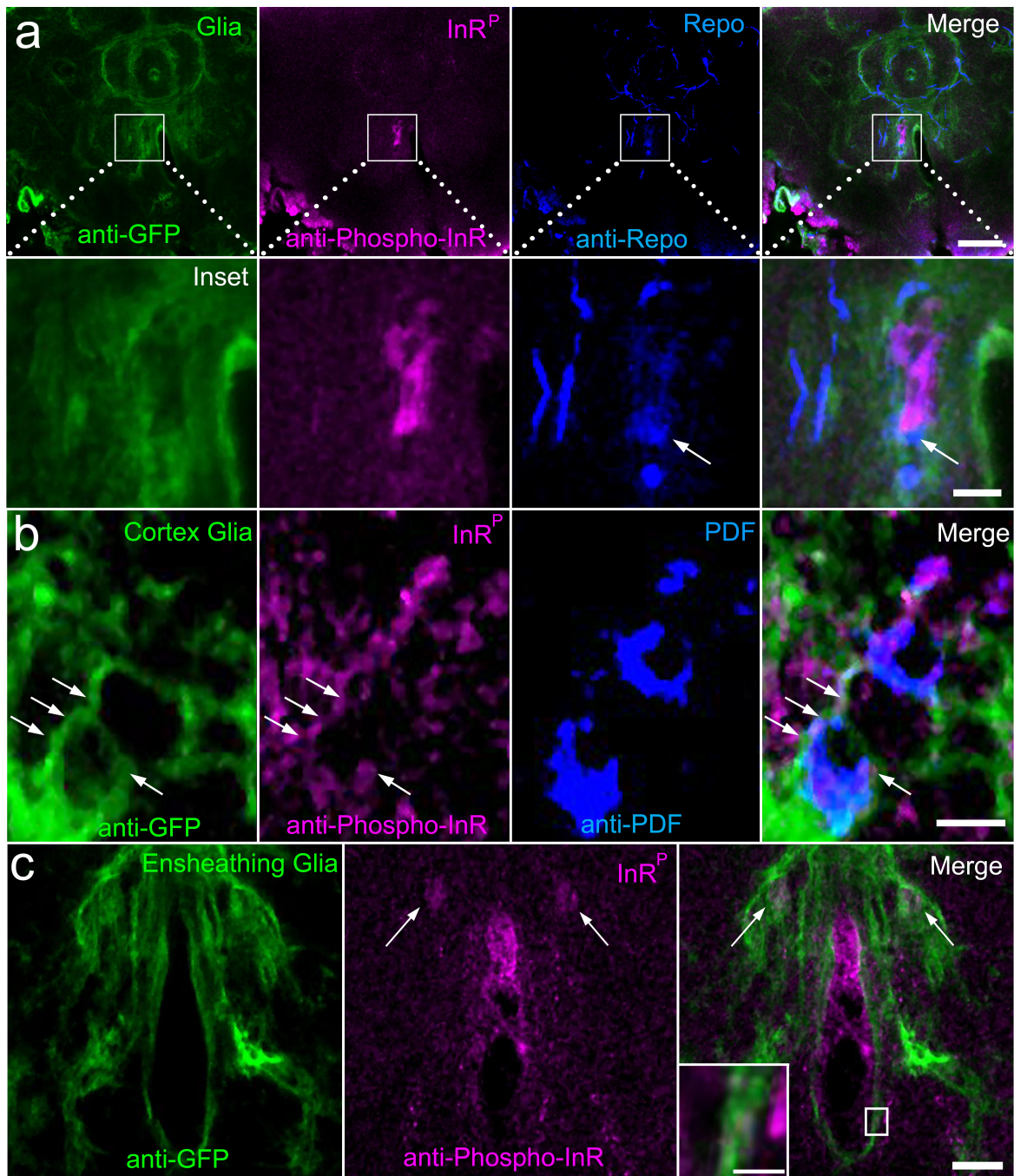
a. Quantification of anti-PDF area (5 DPE) in the proximal subesophageal zone (SEZ, left) and the distal medial bundle (MDBL, right) from the brains imaged in main text Figure 4a. SEZ: CG, two-sided Mann-Whitney,  $p=0.0003$ ,  $5.236 \pm 2.481$   $n=7$  control,  $94.62 \pm 13.93$   $n=8$  *draper*-RNAi; EG, two-sided Mann-Whitney,  $p=0.0034$ ,  $13.19 \pm 11.31$   $n=8$  control,  $58.98 \pm 13.89$   $n=8$  *draper*-RNAi. MDBL: CG, two-sided Mann-Whitney,  $p=0.4126$ ,  $3.305 \pm 2.524$   $n=8$  control,  $9.466 \pm 5.906$   $n=7$  *draper*-RNAi; EG, two-sided t-test,  $p=0.0059$ ,  $6.738 \pm 4.501$   $n=8$  control,  $33.33 \pm 6.844$   $n=8$  *draper*-RNAi. b. Quantification of PDF+ puncta (5 DPE) in the SEZ (left) and MDBL (right) from the same series of experiments. SEZ: CG, two-sided Mann-Whitney,  $p=0.0020$ ,  $2.429 \pm 1.232$   $n=7$  control,  $18.88 \pm 3.573$   $n=8$  *draper*-RNAi; EG, two-sided Mann-Whitney,  $p=0.0006$ ,  $1.25 \pm 0.9955$   $n=8$  control,  $13.88 \pm 2.642$   $n=8$  *draper*-RNAi. MDBL: CG, two-sided Mann-Whitney,  $p=0.4126$ ,  $1.375 \pm 0.9437$   $n=8$  control,  $4.286 \pm 2.643$   $n=7$  *draper*-RNAi; EG, two-sided Mann-Whitney,  $p=0.00373$ ,  $3.625 \pm 2.464$   $n=8$  control,  $12.00 \pm 2.360$   $n=8$  *draper*-RNAi. The cortex glia (CG) transgenic driver control (*R54H02-Gal4/+*) and CG>*draper*-RNAi experimental (*R54H02-Gal4>draper*-RNAi) are shown in black/grey, respectively. The ensheathing glia (EG) driver control (*R56F03-Gal4/+*) and EG>*draper*-RNAi experimental (*R56F03-Gal4>draper*-RNAi) are shown in dark/light blue, respectively. Scatter plots show mean  $\pm$  SEM. Sample size is  $n$ =number of animals. Significance:  $p>0.05$  (not significant N.S.),  $p<0.05$  (\*),  $p<0.01$  (\*\*) and  $p<0.001$  (\*\*\*). Source data for this figure are provided in Source Data file.

**a****Draper****b** **$\alpha$ -Tubulin**

Supplemental Figure 4: Full Western blots from Figure 6a in the main text

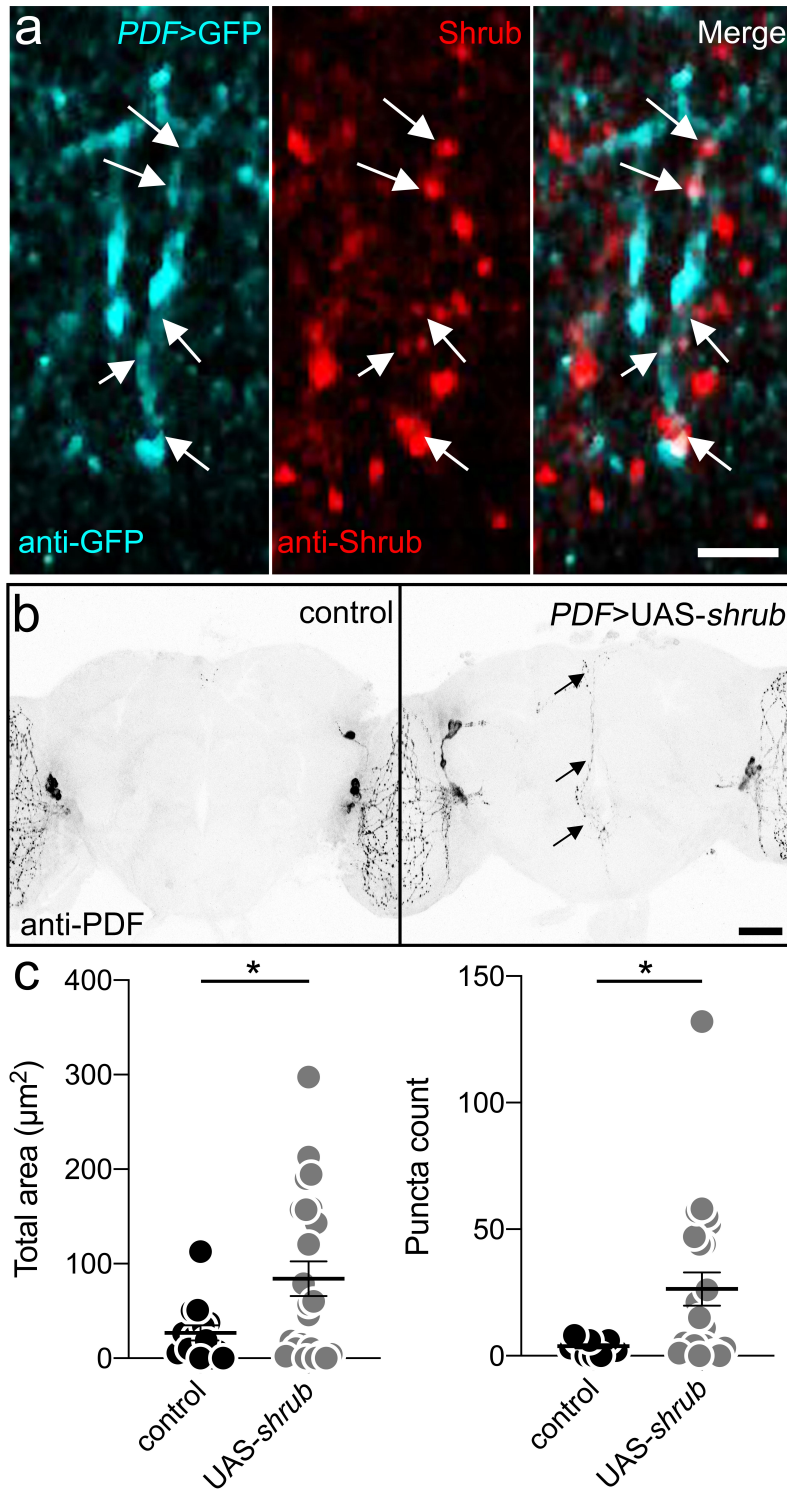
Western blots of whole brain lysates (2 brains per lane, 0 DPE) for control ( $w^{1118}$ ) and *dfmr1* null mutants ( $w^{1118}; dfmr1^{50M}$ ). a. Anti-Draper Western blots with molecular weights listed to the left (kDa). L1 indicates ladder with reduced brightness to show bands. L2 indicates ladder with identical brightness/contrast settings as anti-Draper probe. b. Anti- $\alpha$ -tubulin with molecular weights listed to the left (kDa). L2 indicates ladder with identical brightness/contrast settings as the probe. The Western blot number is indicated, matching Draper and  $\alpha$ -tubulin blots. Boxes indicate bands in main text.





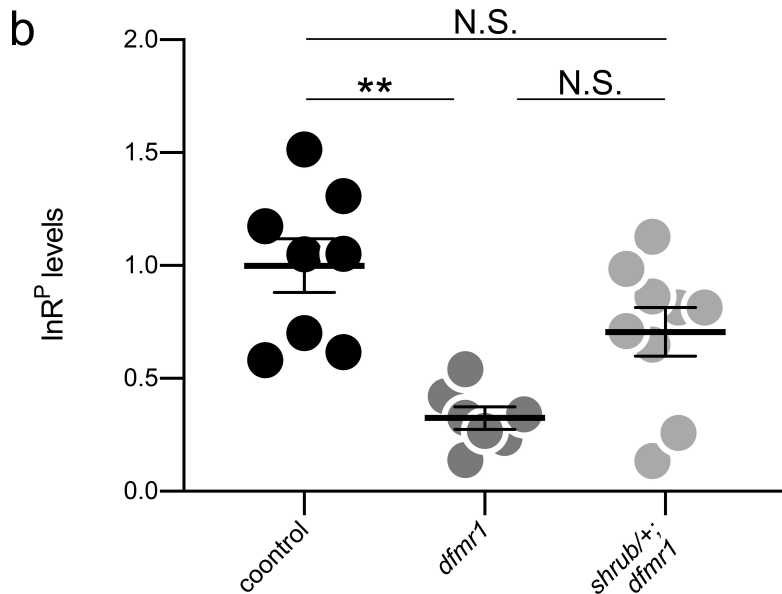
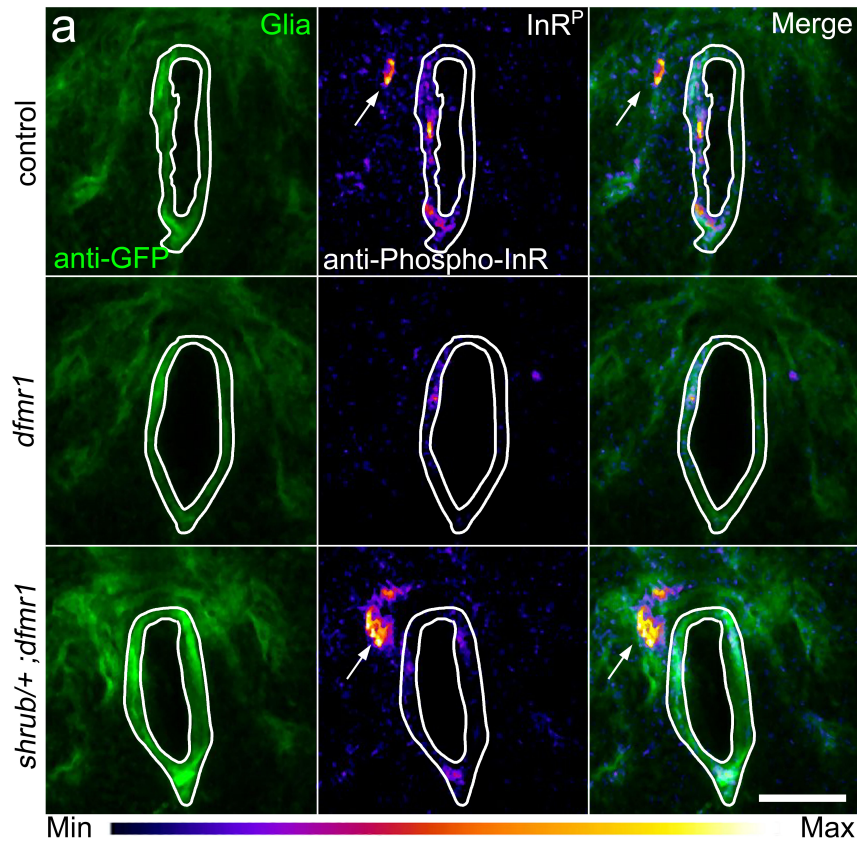
Supplemental Figure 6: InR<sup>P</sup> labeling with anti-Repo glial and glial class GFP markers

a. Central brain slices (2 DPE) with *repo*-Gal4 driven mCD8::GFP in glia (green) co-labeled with anti-InR<sup>P</sup> (magenta) and anti-Repo (blue). Top: Lower magnification images with the merge (right). Scale bar: 40 $\mu$ m. Bottom: High magnification of boxed region in top panel, showing co-localization. Arrow indicates Repo+ cell. Scale bar: 10 $\mu$ m. b. Central brain slices (0 DPE) with mCD8::GFP (green) driven in cortex glia via *R54H02*-Gal4, co-labeled with anti-InR<sup>P</sup> (magenta) and anti-PDF (blue), and the merge (right). Arrows indicate InR<sup>P</sup>+ glial membranes adjacent to PDF-Tri cell body. Scale bar: 10 $\mu$ m. c. Central brain slices (2 DPE) with mCD8::GFP (green) driven in ensheathing glia via *R56F03*-Gal4, co-labeled with anti-InR<sup>P</sup> (magenta), and the merge (right). White arrows indicate InR<sup>P</sup>+ cell bodies. Scale bar: 25 $\mu$ m. Inset is enlarged boxed region. Scale bar: 6 $\mu$ m. Images are representative of two independent experiments.



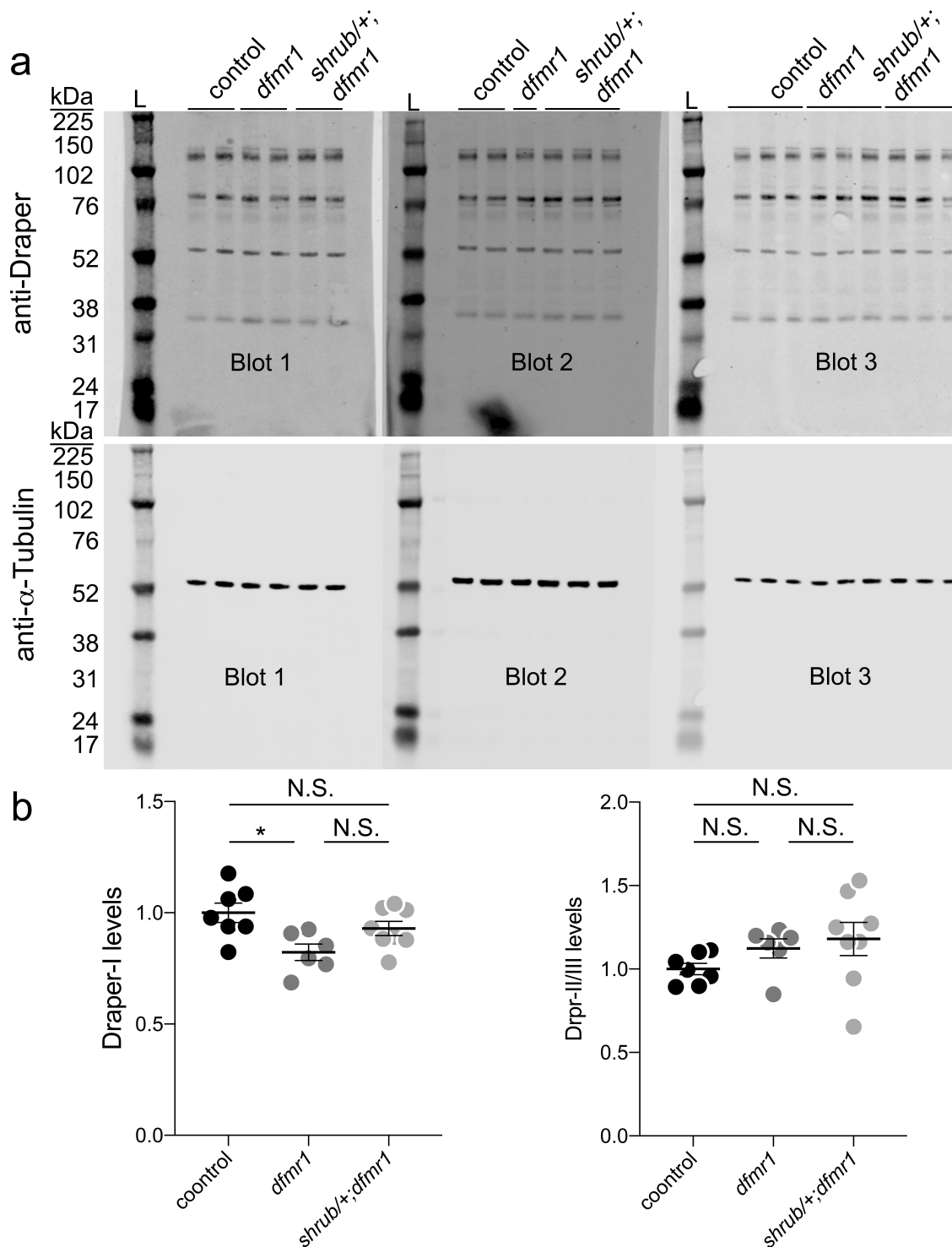
Supplemental Figure 7: Shrub gain-of-function (GOF) roles in PDF-Tri neuron clearance

a. Representative central brain PDF-Tri region images (2 DPE) with *PDF-Gal4>mCD8::GFP* (anti-GFP, cyan, left) and anti-Shrub (red, middle) in PDF-Tri neuron processes, with the merge (right). Arrows indicate thinned PDF-Tri neuron domains co-localized with anti-Shrub puncta. Scale bar: 5 $\mu\text{m}$ . Images are representative of two independent experiments. b. Whole brains (5 DPE) labeled with anti-PDF in transgenic control (*PDF-Gal4/+*, left) and PDF-Tri targeted Shrub overexpression (*PDF-Gal4>UAS-shrub*, right). PDF-Tri neurons (arrows) absent in controls, persist when Shrub is overexpressed. Scale bar: 50 $\mu\text{m}$ . c. Quantification of PDF area (left) and PDF+ puncta (right). Area: Two-tailed t-test,  $p=0.0248$ ,  $26.85\pm 8.134$   $n=14$  control,  $84.22\pm 18.34$   $n=23$  *UAS-shrub*. Puncta: Mann-Whitney,  $p=0.0384$ ,  $3.769\pm 0.7775$   $n=13$  control,  $26.39\pm 6.579$   $n=23$  *UAS-shrub*. Scatter plots show mean  $\pm$  SEM. Sample size is  $n$ =number of animals. Significance shown:  $p<0.05$  (\*). Source data for this figure are provided in Source Data file.



Supplemental Figure 8: FMRP and Shrub interact to drive glial insulin receptor activation

a. Whole brains (2 DPE) co-labeled for glial targeted mCD8::GFP (anti-GFP, green, left), anti-phosphorylated insulin receptor (InR<sup>P</sup>, heat-map intensity, middle) and the merged image (right) in transgenic control (UAS-mCD8::GFP/+; *repo-Gal4*/+, top), *dfmr1* null mutant (UAS-mCD8::GFP/+; *dfmr1*<sup>50M</sup>, *repo-Gal4/dfmr1*<sup>50M</sup>, middle) and heterozygote null *shrub*<sup>+</sup> in the *dfmr1* null (UAS-mCD8::GFP/*shrub*<sup>4</sup>; *dfmr1*<sup>50M</sup>, *repo-Gal4/dfmr1*<sup>50M</sup>, bottom). The white outline indicates glial area used for InR<sup>P</sup> intensity measurements, and arrows indicate glial cell bodies. Scale bar: 25 $\mu$ m. The range indicator below shows InR<sup>P</sup> intensity levels. b. Quantification of normalized InR<sup>P</sup> levels from the images in panel a. Kruskal-Wallis followed by Dunn's multiple comparison test,  $p=0.0030$ ,  $1.00\pm 0.1200$   $n=8$  control,  $0.3246\pm 0.04922$   $n=7$  *dfmr1*;  $p=0.5309$ ,  $1.00\pm 0.1200$   $n=8$  control,  $0.7064\pm 0.1076$   $n=9$  *shrub*;  $p=0.1138$ ,  $0.3246\pm 0.04922$   $n=7$  *dfmr1*,  $0.7064\pm 0.1076$   $n=9$  *shrub*. Scatter plots show mean  $\pm$  SEM. Significance shown:  $p>0.05$  (not significant N.S.) and  $p>0.01$  (\*\*). Source data for this figure are provided in Source Data file.



Supplemental Figure 9: FMRP and ESCRT-III Shrub interact to facilitate Draper expression

a. Full Western blots of whole brain lysates (0 DPE, 2 brains per lane), probing for anti-Draper (top) and anti- $\alpha$ -tubulin (bottom) in the genetic background control ( $w^{1118}$ ), *dfmr1* null mutant ( $w^{1118}; dfmr1^{50M}$ ), and heterozygous null *shrub*<sup>4</sup>/+ in the *dfmr1* null mutant ( $w^{1118}; shrub^4/+; dfmr1^{50M}$ ). The molecular weights are shown to the left (kDa), ladder (L) indicated, and genotypes shown at the top. b. Quantification of Draper-I (left) and Draper-II/III (right) bands normalized to  $\alpha$ -tubulin. Draper-I: Kruskal-Wallis followed by Dunn's multiple comparison test,  $p=0.0160$ ,  $1.00\pm 0.1162$   $n=7$  control,  $0.8227\pm 0.03697$   $n=6$  *dfmr1*;  $p=0.6266$ ,  $1.00\pm 0.1162$   $n=7$  control,  $0.9295\pm 0.03188$   $n=8$  *shrub*;  $p=0.2870$ ,  $0.8227\pm 0.03697$   $n=6$  *dfmr1*,  $0.9295\pm 0.03188$   $n=8$  *shrub*. Sample size is  $n$ =number of independent protein extractions (2 brains per extraction). Scatter plots show mean  $\pm$  SEM. Significance shown:  $p>0.05$  (not significant, N.S.) and  $p<0.05$  (\*). Source data for this figure are provided in Source Data file.